International Journal of Architecture and Urban Development
Vol. 15, No. 4, P 91- 112 Autumn 2025

E-ISSN 2345-2331
Applied Research Article
DOI: 10.71711/ijaud.2025.1219518

Comparative Analysis of Solar Rights from Neighborhood to Building Scale (Case Study: Yousefabad, Tehran)

[1*]Niloufar Mosalmanfarkoosh, [2]Hadi Pendar, [3] Pantea Alipour Kouhi, [4] Niusha Mosalmanfarkoosh
[1*] Department of Urban Design, Faculty of Architecture and Urban Planning, Iran University of Art, Tehran, Iran.
[2] Department of Urban Design, Faculty of Architecture and Urban Planning, Iran University of Art, Tehran, Iran.
[3] Department of Urban Development, SR.C, Islamic Azad University, Tehran, Iran.
[4] Department of Architecture, Faculty of Islamic-Iranian Arts, Farshchian Branch, Islamic Azad University, Tehran, Iran.

Recieved 29.09.2025; Accepted 27.10.2025

ABSTRACT: Rapid urbanization has accelerated recently, bringing environmental and equity challenges, particularly in solar and daylight access. In Yousefabad (District 6, Tehran), rapid densification under current height codes threatens residents' daylight access. Accordingly, this study addresses these challenges by evaluating solar access and developing morphology-based height regulations that safeguard residents' right to sunlight, focusing on efficiency, equity, and the trade-offs between them in solar performance. This study adopts an applied, quantitative approach to evaluate solar radiation (SR), sunlight duration (S_H), and sky view factor (SVF) across three spatial scales—macro (neighborhood), meso (urban block), and micro (building) —to derive an optimized height. The workflow combines GIS-based analysis, parametric modeling in Rhinoceros, and environmental simulations in Ladybug and Honeybee, while a genetic algorithm optimizes design scenarios and Gini coefficients (G_SR, G_SH, G_SVF) quantify equity in solar access. Results indicate that current height codes restrict daylight and solar access compared to the optimized scenario. Based on the equity indicator and Gini coefficients, the optimized scenario reduced G_SR, G_SH, and G_SVF by roughly 16%, 20%, and 11%, while increasing mean SR, sunlight hours, and SVF by about 15–20%. These outcomes defined block-specific height bands and guidelines to help planners and policymakers enhance solar equity in dense areas. The main innovation lies in a unified analytical–optimization framework linking neighborhood, block, and building-scale evaluations. The proposed framework links urban form to solar equity, demonstrating that balanced height and density improve solar access in dense cities.

Keywords: *Solar Access; Right-to-Light; Urban Morphology; Sky View Factor (SVF); Genetic Algorithm; BIPV; UBEM.*

INTRODUCTION

Urbanization trends reveal that cities, as complex and dynamic systems, play a major role in global energy consumption and carbon emissions (Bentley et al., 1985; Moonen et al., 2012; Amado et al., 2016). With growing urban populations, energy demand and emissions are expected to intensify, underscoring the need to shift from fossil fuels toward sustainable, renewable, and smart energy systems (York & Bell, 2019; Thellufsen et al., 2020; Poggi & Amado, 2024). Among renewable sources, solar energy is particularly significant for its capacity to improve economic efficiency, public health, and overall well-being when widely implemented (Okeil, 2010; Smith et al., 2025). Urban morphology critically shapes building energy performance by affecting daylight access and microclimatic conditions (Ratti et al., 2005; Wang et al., 2025).

Many studies confirm that the physical form of residential areas strongly influences urban energy efficiency (Cheng et al., 2006; Liu et al., 2023; Rostami et al., 2024). Yet, no consensus exists on the most effective morphological patterns for solar use. In practice, planners emphasize land use and density, while the energy impacts of form remain underexplored (Ratti et al., 2005; Oh et al., 2021; Elaouzy, 2025). Conventional approaches to energy efficiency focus on insulation and thermal mass, often neglecting form-related parameters. This research, therefore, seeks to bridge the gap between morphological form and equitable solar access by developing a multi-scale analytical framework. To address this research gap, the study formulates the following research questions:

*Corresponding Author Email: n.mosalman@student.art.ac.ir ORCID: 0009-0003-5659-6173

- How does urban densification affect residents' equitable access to solar radiation and daylight across macro, meso, and micro scales?
- To what extent do current FAR and height codes in Tehran align with principles of solar rights and daylight equity?
- How can optimization frameworks (GA-based) generate morphology-informed height regulations that balance density with solar access?

This study is framed within a broader normative and regulatory context that recognizes access to sunlight as both a spatial and environmental right. The concept of solar rights, rooted in the right-to-light principle, frames daylight as a normative entitlement rather than merely a design variable. In Tehran, existing planning codes emphasize quantitative density through Floor Area Ratio (FAR) and height limits while overlooking the equity dimension of solar access. In contrast, international frameworks such as the UK Right to Light Act and European daylight standards (e.g., EN 17037) integrate solar access directly into urban regulations, demonstrating how rights-based principles can be translated into measurable spatial criteria. Building on these precedents, this study operationalizes the notion of solar equity by tailoring morphological design parameters to Tehran's dense urban context. Equity here is treated as a quantifiable dimension of environmental performance, assessed via the Gini coefficient and variance derived from three solar indicators, solar radiation (SR), sunlight duration (S_H), and sky view factor (SVF), to capture how urban form governs the fair distribution of daylight benefits among residents.

Literature Review

The concept of solar rights, closely linked to the right to light, has evolved from early architectural ethics into a spatial and regulatory concern in contemporary urban design. It frames access to sunlight as a matter of environmental equity, emphasizing its importance for daylight availability, public health, and thermal comfort (Rostami et al., 2024). Recent studies have expanded this perspective by examining how urban morphology directly affects solar access and energy performance (Wang et al., 2024). Factors such as building orientation, block configuration, and façade typology determine how sunlight is distributed across dense urban environments (Morganti et al., 2017; Shi et al., 2017). Consequently, research in urban morphology and environmental design increasingly views solar rights not merely as a legal or ethical concept but as a quantifiable urban performance criterion that links spatial form with environmental equity.

From a policy perspective, the implementation of solar rights varies widely across contexts. In the United Kingdom, the Right to Light Act (1959) legally protects daylight access for existing buildings, treating sunlight as a property entitlement that can limit new development. Internationally, the IEA Solar Access Guidelines (2013) and the European Daylight Standard (EN 17037) integrate solar access into planning systems through measurable criteria for daylight sufficiency, view quality, and exposure duration. These frameworks demonstrate how solar rights have evolved from normative principles into performance-based planning tools. However, in many Middle Eastern contexts, including Tehran, current regulations still prioritize quantitative density metrics such as Floor Area Ratio (FAR) and height limits, with little attention to solar equity or daylight fairness.

Building on these theoretical and policy insights, recent studies have examined how solar access and energy performance can be assessed across different spatial scales. Research spans from neighborhood- and city-level analyses of urban morphology to block- and building-scale evaluations of form, orientation, and density. Various simulation and optimization tools have

Table 1: Studies on solar-access and energy-performance across macro/meso/micro scales. Key authors, methods/algorithms, tools, and findings.

Authors	Method/Algorithm	Tools	Results
Macroscale_Neighborhood / City			
Lobaccaro et al., 2012	MATLAB algorithm	RADIANCE-DAYSIM, a dynamic simulation tool	Integrated Sustainable Design approach PV modules and Solar thermal collectors in the building envelopes
Shi et al., 2017	Differential evolution	City Energy Analyst (CEA)	optimization for energy-driven urban design
Morganti et al., 2017	Energy data analysis	Ecotect and heliodon	Urban morphology indicators gross space index, floor space index, average building height, volume to area ratio, building dimensions ratio, and sky factor of building factors Gross space index
Sarralde et al., 2015	Generic model	ArcGIS ArcMap	Different scenarios of urban morphology are analyzed, and the variables of urban form are tested.
Lobaccaro et al., 2019	DAYSIM-based hourly Cumulative ,method sky method simulation modeling	Rhinoceros3D/Grasshopper/Honeybee DIVA Revit	Results show that, depending on urban morphology and building shapes, PV systems can cover more than 40% of a building's total energy needs.

Continiue of Table 1: Studies on solar-access and energy-performance across macro/meso/micro scales. Key authors, methods/algorithms, tools, and findings.

Authors	Method/Algorithm	Tools	Results
		Mesoscale_Urban Blocks	
Kanters & Horvat, 2012	-	Ecotect	Energy efficiency simulation of urban blocks/ The effect of morphology on the potential of SR energy consumption decreased by 10%-70%
Doherty et al., 2009	Parametric modeling -MATLAB	Energy Plus 8- AutoCAD	Morphological factors, including density, species, and urban form
Vartholomaios, 2015	combines the RSB typology with solar envelopes	Rhinoceros3D/ Grasshopper	The presented construction method of the RSB envelope is transferable to different climatic and development conditions.
Vermeulen et al., 2018	Evolutionary Algorithms	ENVI-MET	urban models for optimization of passive solar irradiation
Pakzad & Salari, 2018	Computational Design Environment Simulation	Grasshopper and Ladybug Tools	Solar Space Envelope analysis of the stability of the urban block block, including size-length, structure- orientation
Shi et al., 2021	Energy Simulation	Grasshopper and Rhino	Typology of native blocks The optimal form of the residential block
Mirzabeigi & Razkenari, 2022	multi-phase optimization framework- physics-based simulation	computational workflow with various simulation tools	The energy efficiency of each alternative was compared
Geng et al., 2024	Regression Analysis multi-objective genetic optimization	-	Analytical concepts that shed light on the intricate relationship between urban morphologies and photovoltaic potential.
		Microscale_Buildings	
Ratti et al., 2003	Parametric modeling	-	building patterns with courtyards as optimal patterns
Tuhus-Dubrow et al., 2010	Genetic algorithm	MATLAB	Optimize building envelope design for residential buildings
Freitas et al., 2015	Algorithm SOL LiDAR data	GRASS r.sun	Solar energy potential on roofs and façades in an urban landscape
Amado et al., 2016	Parametric modeling Cellular Automata (CA)-GAS	-	Intelligent texture design Improving the energy efficiency of cities - solar energy
Stasinopoulos, 2018	examines the volume of the solar envelope	AutoCAD	compares the effect of factors on the size of solar envelopes on a variety of land parcels
Ferrando et al., 2020	Evaluate energy scenarios	Bottom-up physics-based UBEM tools	Barriers to the adoption of UBEM tools include the need for a standardized ontology, a common three-dimensional city model, a standardized data-collection procedure, and a standardized set of test cases.
De Luca et al., 2021	Computational Design Environment Simulation	Grasshopper and Ladybug Tools	Direct access to sunlight - various blocks - ratio of the surface receiving radiation
Zhao et al., 2023	Integrated evaluation framework	-	Proposing an integrated evaluation framework for BIPV (Building-integrated photovoltaics)

been used to explore how design parameters influence solar radiation, daylight availability, and overall energy efficiency. Table 1 summarizes key contributions across macro, meso, and micro scales, outlining their main methods, tools, and findings as the basis for this study.

As shown in Table 1, previous studies have examined solar access and energy performance across different spatial scales, highlighting the strong influence of urban form on environmental outcomes. At the macroscale, research links city morphology with renewable energy potential, using GIS-based and simulation tools to assess how density, height, and layout affect solar availability (Lobaccaro et al., 2012; Shi et al., 2017). At the mesoscale, block-level studies explore how orientation, compactness, and site coverage shape solar radiation and daylight distribution (Kanters & Horvat, 2012; Vartholomaios, 2015). Microscale analyses focus on building geometry and envelope design, showing that courtyard and solar-block forms achieve higher performance in hot-arid

climates (Ratti et al., 2003; Amado et al., 2016).

Although previous studies have linked urban form to solar performance, their comparative effects across scales remain underexplored. Each scale shows distinct spatial and climatic trade-offs. At the macroscale, compact forms improve land use but reduce solar access through shading. At the mesoscale, block orientation affects the balance between solar radiation (SR) and sky view factor (SVF). At the microscale, façade depth and spacing influence sunlight duration (S_H) and glare control, varying by climate. Deeply recessed façades suit warm-arid regions like Tehran, while shallow ones perform better in colder climates. These findings reveal scale-specific mechanisms and emphasize the need for comparative, data-driven evaluation. Table 2 summarizes the main indicators at the macro (city), meso (block), and micro (building) levels, integrating both physical and climatic dimensions.

As summarized in Table 2, the selected indicators capture both the physical characteristics of urban form and the climatic

Table 2: Morphological and solar-access indicators by scale. Notes: SR (kWh/ yr), S_H (h/yr), SVF (%).

Macroscale_Neighborhood / City			
	Authors		
Physical Dimension		Climatic Dimension	
Neighborhood Orientation (NO)	Morganti et al., 2017 Sarralde et al., 2015	Solar Radiation (SR)	Shi et al., 2017
Form of the Neighborhood (NF)	Lobaccaro et al., 2019 Sarralde et al., 2015	Duration of Solar Radiation (S_H)	
Macroscale Density (MD)	Morganti et al., 2017 Sarralde et al., 2015		
Neighborhood Typology (ND)	Lobaccaro et al., 2019 Sarralde et al., 2015		
Average block size (BZ_mean)	Shi et al., 2017		
Mass to space ratio (M2S)	Morganti et al., 2017 Sarralde et al., 2015		
Average Height (H)	Morganti et al., 2017		
Average floor Number (FN_mean)	-		
Mesoscale_Urban Blocks			
Physical Dimension		Climatic Dimension	
Block Orientation (BO)	Pakzad & Salari, 2018 Stasinopoulos, 2018 Mirzabeigi & Razkenari, 2022	Solar Radiation (SR)	Vartholomaios, 2015
Typology of blocks (T)	Doherty et al., 2009 Mirzabeigi & Razkenari, 2022	Duration of Solar Radiation (S_H)	
Dimensions and Size (S)	Pakzad & Salari, 2018 Stasinopoulos, 2018	Index of visibility to sky (Sky View)	
Density (D)	Doherty et al., 2009 Mirzabeigi & Razkenari, 2022		
Average Block Height (BH_mean)	Pakzad & Salari, 2018		
Average floor Number (FN_mean)	Geng et al., 2024		
Mean of surface area (SA_mean)			
Total façade Area (FA_Total)			
Mean of façade area (FA_mean)			
Total Surface Area (SA_Total)			
Microscale_Buildings			
Physical Dimension		Climatic Dimension	
Buildings Orientation (O)	De Luca et al., 2021 Amado et al., 2016	Solar Radiation (SR)	Tuhus-Dubrow & Krarti, 2010

Continiue of Table 2: Morphological and solar-access indicators by scale. Notes: SR (kWh/ yr), S_H (h/yr), SVF (%).

Microscale_Buildings		
Typology of individual buildings (T)	Tuhus-Dubrow & Krarti, 2010 Zhao et al., 2023 Amado et al., 2016	
Dimensions and Size (S)	Tuhus-Dubrow & Krarti, 2010	
Building Height (H)	Tuhus-Dubrow & Krarti, 2010 Zhao et al., 2023	
Average Building Height (BH_mean)	Geng et al., 2024	
Floor Area Ratio_FAR/Floor Space Index (FSI)		
Total Surface Area (TSA)		
Mean of façade area (FA_mean)		
Building Density (BD)	Tuhus-Dubrow & Krarti, 2010 Amado et al., 2016	Duration of Solar Radiation (S_H)
Transparent to Non-trans Surfaces Ratio(T2NT)	Tuhus-Dubrow & Krarti, 2010	
Openings (OP)		
Internal Shading (IS)	De Luca et al., 2021 Ratti et al., 2003	
Mass to space ratio (M2R)	De Luca et al., 2021	
Numbers and types of openings	Tuhus-Dubrow & Krarti, 2010	
The type of materials used	-	
Material color	-	

variables that influence solar performance at different scales. Among the climatic indicators, three core variables are employed to link urban morphology with solar-access equity:

- Solar Radiation (SR) measures the total solar energy received on urban surfaces (kWh) and reflects the potential for passive heating, daylighting, and solar energy generation. It varies with building height, orientation, and shading.
- Sunlight Duration (S_H) represents the total time façades and open spaces receive direct sunlight, indicating daylight availability and the consistency of solar exposure across urban areas, key to ensuring equitable solar access.
- Sky View Factor (SVF) measures the visible portion of the sky from a point, indicating spatial openness. Low values reflect dense, enclosed areas, while high values denote open forms with better daylight, ventilation, and heat dissipation.

Building on these insights, the study develops a conceptual framework, as illustrated in Figure 1, that links morphological parameters with key solar-performance indicators (SR, S_H, and SVF) and equity outcomes, establishing a connection between form analysis and policy-oriented design guidance.

Although the influence of urban morphology on solar performance is well established, its multi-scalar dynamics remain insufficiently examined. In Tehran's densifying urban fabric, particularly in Yousefabad, increasing FAR and vertical expansion have intensified conflicts between development intensity and daylight access. To address these challenges, this study presents a data-driven, multi-scale framework (illustrated in Figure 2) that integrates simulation and GA-based optimization to evaluate and enhance solar-access equity within height–density configurations. This study introduces a data-driven, multi-scale optimization framework linking urban morphology with solar accessibility and equity. Unlike earlier single-scale approaches, it:

- Integrates simulation and GA-based optimization to generate height configurations that balance densification with solar equity.
- Bridges macro-, meso-, and micro-scale analyses within a single analytical structure, enabling cross-scale understanding of solar distribution.
- Quantifies equity in solar access using measurable performance indicators (SR, S_H, SVF) rather than qualitative evaluation.
- Translates analytical results into design guidance, providing a reproducible method for developing solar-informed height codes.

Together, these innovations establish a replicable workflow that connects form, performance, and equity, offering planners practical tools to align urban growth with daylight quality and environmental sustainability.

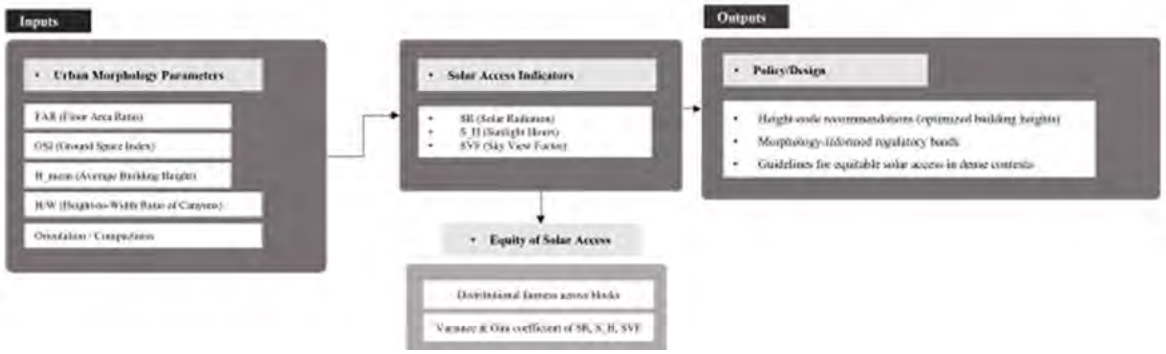

Fig. 1: Conceptual framework linking urban morphology to solar-access and equity. Pathway from form parameters to indicators and equity metrics (variance, Gini).

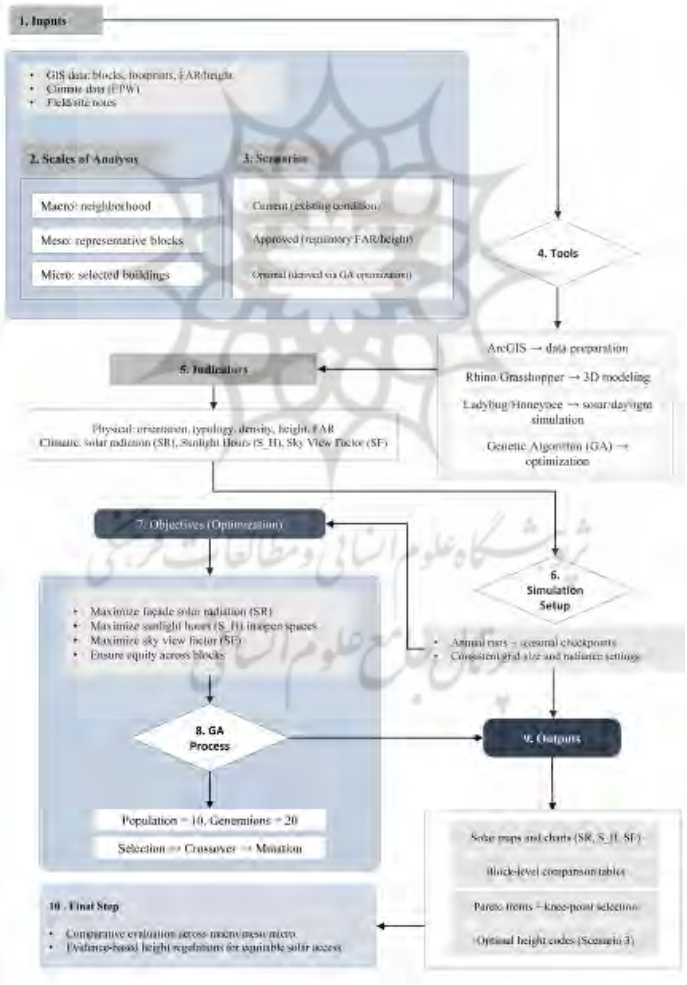

Fig. 2: Integrated workflow for multi-scale simulation and GA-based optimization (GIS → Rhino/Grasshopper → Ladybug/Honeybee → GA)

MATERIALS AND METHODS

This research framework, as shown in Figure 2, encompasses three main stages:

- Stage 1: Morphological and solar parameters are defined across three scales, macro (neighborhood/city), meso (urban block), and micro (building), using indicators that capture both geometric features (orientation, density, height, typology) and solar attributes (SR, S_H, SVF, façade exposure).
- Stage 2: Three development scenarios — Current, Approved, and Optimal — are simulated and compared. The Optimal scenario, generated through GA-based optimization, maximizes solar access and links empirical observation with predictive modeling.
- Stage 3: A comparative evaluation identifies which configuration best supports solar access, daylight availability, and equitable light distribution, revealing trade-offs between densification and solar rights to inform data-driven planning and design decisions.

To ensure methodological coherence, the analytical framework was developed in direct alignment with the research questions introduced in the Introduction. Accordingly, the study addresses its main objective through four sub-questions that guide the multi-scalar analysis and scenario simulations:

1) Macroscale: How do neighborhood orientation, density, and typology affect the distribution of solar radiation (SR) and sunlight duration (S_H)?

2) Mesoscale: How do variations in block orientation, floor area ratio (FAR), and open-space configuration influence SR, S_H, and sky view factor (SVF) under different development scenarios?

3) Microscale: Which building characteristics (e.g., height, FAR, façade transparency, and active façades) most strongly determine daylight penetration and solar benefits?

4) Optimization: How can a genetic algorithm (GA) generate an optimized morphological configuration that balances densification pressures with equitable solar accessibility?

Study Area and Datasets

The Yousefabad neighborhood in District 6 of Tehran, situated on a northwest hillside, has undergone substantial morphological transformation under economic and developmental pressures that have intensified urban density. It comprises three block clusters with distinct geometry and orientation, characterized by linear and semi-regular forms, limited green areas such as Shafaq Park and Asadabadi Square, and predominantly mid-rise residential structures, with higher-rise developments concentrated along the Asadabadi corridor. The prevailing northeast–southwest orientation enhances solar access, while variations in height and spacing generate diverse shading patterns, making Yousefabad a representative case for analyzing density-driven impacts on solar accessibility, as illustrated in Figure 3.

The study area was examined across three spatial scales: the macroscale for neighborhood morphology and density; the mesoscale for block configuration and façade exposure; and the microscale for building geometry and solar access. Each scale is detailed in the following subsections with its analytical scope and datasets.

- Macroscale: Yousefabad Neighborhood

At the macroscale, the Yousefabad neighborhood has a compact urban fabric defined by northeast–southwest and northwest–southeast orientations that shape radiation and shading patterns. Variations in block geometry create alternating dense and open zones, while limited open spaces such as Shafaq Park and Asadabadi Square serve as key solar catchment areas. The mid-rise profile and higher-rise developments along the Asadabadi corridor, as shown in Table 3, increase mutual shading and reduce façade solar exposure.

As summarized in Table 3, the neighborhood exhibits a dominant linear typology (M2S = 1.17; density = 250%), moderate height (≈ 17 m), and introverted block arrangements that collectively define its macro-scale solar performance potential.

- Mesoscale: Urban Blocks

At the mesoscale, the blocks surrounding Asadabadi Square exhibit diverse spatial layouts and interactions with adjacent open areas. These blocks are predominantly residential, and their classification according to specific morphological criteria, as illustrated in Figure 3(b), provides the basis for defining this neighborhood unit as the mesoscale of the study. To capture these variations, six representative blocks were selected for analysis. Their characteristics, including orientation, density, height, and number of floors, are summarized in Table 4.

If ongoing construction activities in the central area of the Yousefabad neighborhood (mesoscale) continue, and the approved FAR regulations are applied, the residential blocks are expected to undergo significant changes in both floor area ratio (FAR)13 and overall morphology. Mosalmanfarkoosh, 2025(. To capture these dynamics, two scenarios were defined; the first represents the current state of the neighborhood, while the second reflects the anticipated conditions following the implementation of the approved FAR regulations, as illustrated in Figure 4 and summarized in Table 5.

To assess the impact of current and approved regulations, six representative blocks in Yousefabad were analyzed under two scenarios, as detailed in Table 5.

As shown in Table 5, planned modifications and potential building extensions are expected to increase both FAR and building height within the study area. The current average height of about 4.1 floors is projected to rise to five or six, with unauthorized additions likely pushing FAR beyond official limits.

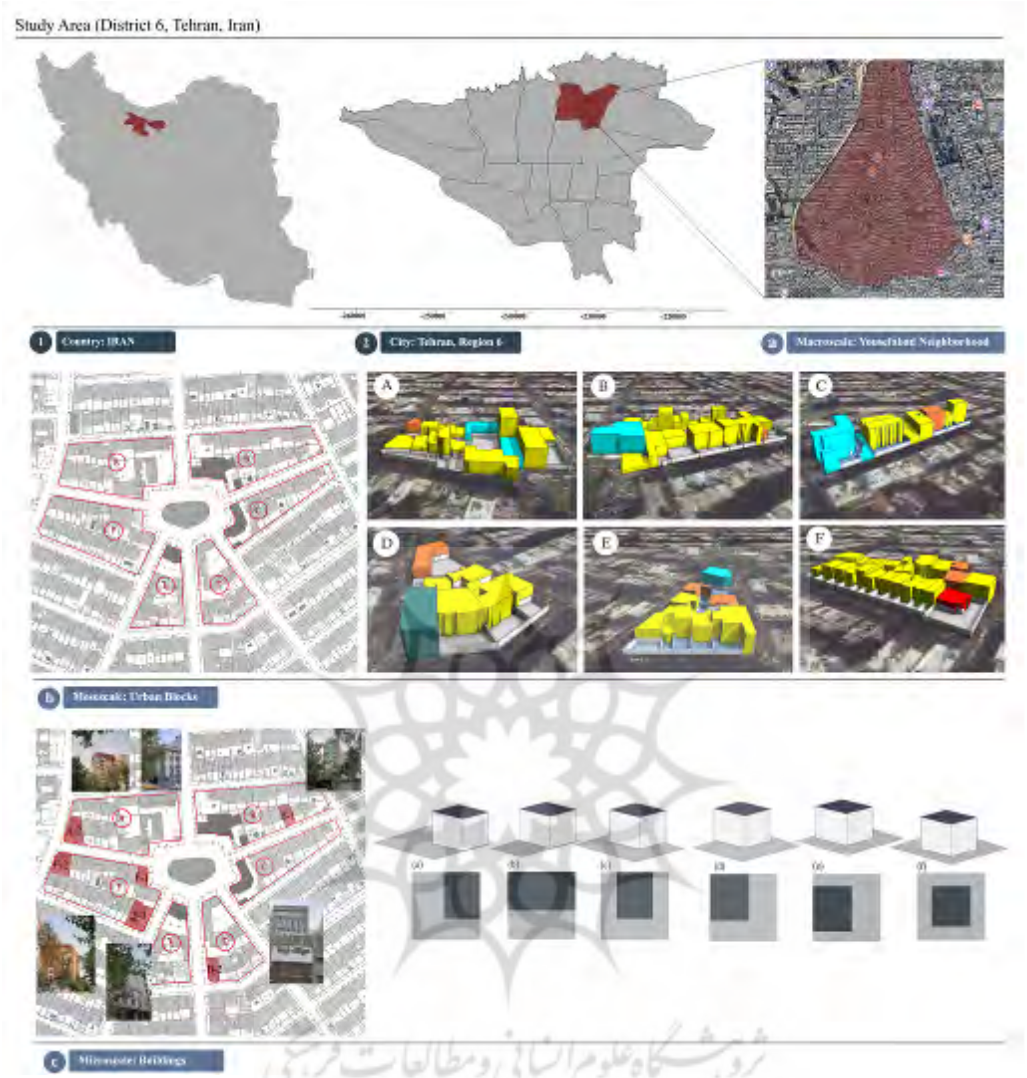

Fig. 3: Study area and analysis hierarchy. (a) Scope hierarchy (neighborhood → block → building); (a) Macroscale: Yousefabad Neighborhood; (b) Mesoscale: Urban Blocks; (c) Microscale: Buildings.

Table 3: Macroscale indicators for Yousefabad neighborhood.

Criteria	Description / Value
Neighborhood Orientation[1]	Eastern half: NW[2]-SE[3] ;Western half: NE[4]-SW[5]
Form of the Neighborhood[6]	Regular Morphology - Introverted Center Blocks
Macroscale Density[7]	250%
Neighborhood Typology[8]	Linear Regular (dominant); Center of the Intra-Spatial (semi-regular spatial)
Average block size (BZ_mean)[9]	7840.94 m2
Mass to space ratio (M2S)[10]	1.17
Average height (H)[11]	16,906 m
Average floor Number (FN_mean)[12]	floors 4.83

Table 4. Mesoscale characteristics of representative blocks (A–F).

Factors / Blocks	Block A	Block B	Block C	Block D	Block E	Block F
Building Orientation (O)	N-S	N-S	NW-SE	NW-SE	N-S	NE-SW
Typology (T)	Semi-regular -linear	Semi-regular -linear	linear	Semi-regular -linear	Semi-regular -linear	linear regular-ize
Area (A) m²	5898.87 m²	9353.98 m²	5146.74 m²	5073.18 m²	4483.56 m²	8541.88 m²
Density (D) %	52%	61%	60%	58%	60%	60%
Building Height_mean (BH) m	13.44 m	16.52 m	15.5 m	15 m	18.2 m	15.4 m
Floor Number_mean (FN)	3.84	4.72	4.3	5	5.2	4.4

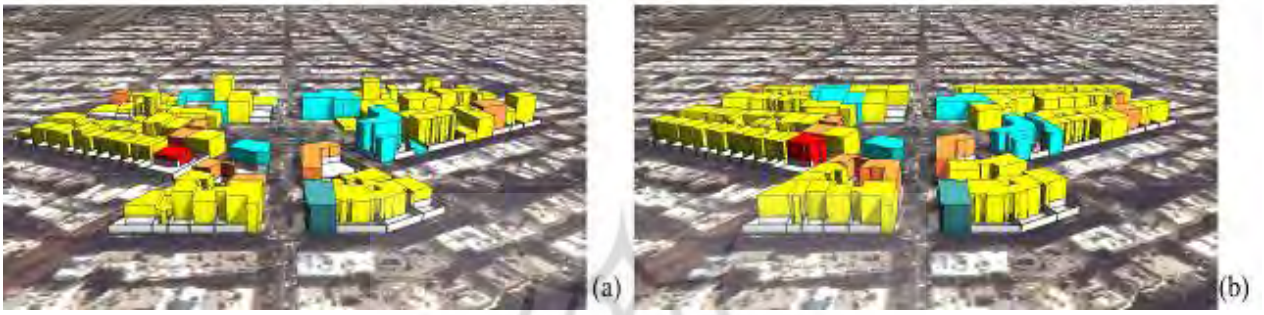

Fig. 4: 3D representations of Scenario 1 (current) and Scenario 2 (approved). (a) Existing morphology; (b) densified morphology under approved FAR.

Table 5. Morphological comparison: Scenario 1 vs. Scenario 2 (mesoscale).

Building Orientation			Typology					Area		(%) FAR				
Block	-	A	B	C	D	E	F	-	A	B	C	D	E	F
Scenario 1	Unchanged	L-C[15]	L[16]	L	L- C	L-C	L	Unchanged	52%	61%	60%	58%	58%	60%
Scenario 2	Unchanged	L	L	L	L	L	L	Unchanged	58%	64%	61%	63%	63%	61%

Building Height_mean (m)							Floor Number_mean						GOP[14]					
Block	A	B	C	D	E	F	A	B	C	D	E	F	A	B	C	D	E	F
Scenario 1	13.4	16.52	15.05	15	18.02	15.4	3.84	4.72	4.3	5	5.2	4.4	OSC[17]	OSS[18]	OSS	OSC	OSS	OSS
Scenario 2	14	18	16	16	19	16	4	5.14	4.5	4.5	4.5	4.5	Open space plots in the south					

Density (%)						
Block	A	B	C	D	E	F
Scenario 1	312%	290%	258% 264%	287%	240%	
Scenario 2	360%	300%	300% 300%	300%	290%	

- Microscale: Buildings

At the microscale, six representative residential buildings were selected and categorized into distinct typologies based on key morphological indicators, as listed in Table 6.

As summarized in Table 6, the six representative buildings exhibit distinct typologies and geometries. Each case was analyzed for key geometric parameters. Figure 3(c) illustrates their spatial distribution and typological diversity, enabling assessment of how micro-scale morphology influences the intensity and uniformity of solar exposure across building forms.

Climatic Characteristics and Analytical Basis

The climatic data for all EnergyPlus and Radiance simulations were obtained from the official Tehran weather file (IRN_Tehran.718400_IWEC.epw), corresponding to 35.69° N, 51.31° E, and an elevation of approximately 1,190 m above sea level. This dataset, representing the Mehrabad synoptic station, ensures that solar geometry, air temperature, and radiation parameters accurately reflect the local climatic conditions of

Table 6. Microscale building characteristics (six samples).

Building Code	Typology	Area (m^2)	Height (m)	FAR	Total Surface Area	T2NT	Mass to Space Ratio	Number of Openings
A-2	Three FRS[19]	706.14 m2	21 m	69%	729.65 m2	2.75	2.53	56
B-1	One FRS	375.93 m2	24 m	62%	1252.49 m2	0.28	1.63	32
D-2	Two FRS	382.7 m2	15 m	61%	657.30 m2	3.25	3.1	110
F-1	Two FRS	282.8 m2	9 m	75%	1034.21 m2	0.95	3	12
F-2	Three FRS	679.74 m2	18 m	% 52	1224.02 m2	0.7	1.08	60
F-3	Two FRS	1007.83 m2	18 m	% 35	859.20 m2	0.8	0.53	66

Tehran. To capture annual solar variations, the simulations were performed for a full year (8,760 hours), supplemented by three representative reference days corresponding to seasonal extremes and a temperate midpoint:

- 21 March (Vernal Equinox): represents the spring equinox, moderate solar altitude, and ambient temperature.
- 21 June (Summer Solstice): corresponds to the warmest period of the year, the highest solar altitude, and maximum solar radiation intensity.
- 21 December (Winter Solstice): marks the coldest period of the year, the lowest solar altitude, and the minimum ambient temperature.

Each reference day was simulated over a 24-hour diurnal cycle using an hourly timestep, while the annual simulation (8760 hours) was conducted to calculate cumulative solar radiation and total sunlight hours across the neighborhood, block, and building scales. The Radiance simulation parameters were defined as ab = 6, ad = 2048, as = 512, ar = 128, aa = 0.1, ps = 0.5, and pj = 0.9. To maintain spatial accuracy and consistency across scales, the grid resolution was explicitly set to macro = 5 m, Meso = 2 m, and micro = 0.5 m. Radiance settings followed standard, convergence-tested parameters (ab = 6, ad = 2048, as = 512, ar = 128, aa = 0.1, ps = 0.5, pj = 0.9) across all scales. A concise summary of the key climatic and simulation parameters is provided below:

- Location: Tehran, Iran
- Latitude / Longitude / Elevation: 35.69° N / 51.31° E / 1190 m a.s.l.
- Weather File: IRN_Tehran.718400_IWEC.epw
- Simulation Type: Annual (8760 h) + 3 reference days
- Reference Days: 21 March (Vernal Equinox), 21 June (Summer Solstice), 21 December (Winter Solstice)
- Timestep: 1 hour
- Radiance Parameters: ab = 6; ad = 2048; as = 512; ar = 128; aa = 0.1; ps = 0.5; pj = 0.9
- Sampling Grid Size: Macro = 5 m; Meso = 2 m; Micro = 0.5 m
- Data Source: EnergyPlus / Ladybug & Honeybee (Tehran IWEC)

The distribution of solar radiation across the study area varies noticeably from west to east. The total annual radiation received ranges from approximately 35 to over 66 kWh, with direct radiation showing significantly higher values than diffuse radiation. Diffuse radiation generally ranges from 24 to 30 kWh, while direct radiation peaks at 110°-250° azimuth, reaching values of 30-48 kWh.

Tools and Techniques

A combination of GIS, parametric, and simulation tools ensured a structured and reproducible workflow. As shown in Figure 5, ArcGIS generated 3D block models and morphological indicators, while Rhinoceros–Grasshopper with Ladybug and Honeybee simulated solar radiation (SR), sunlight hours (S_H), and sky view factor (SVF) across scales. The outputs were then integrated into a Genetic Algorithm (GA) to optimize block configurations and solar accessibility.

Data Collection

The Yousefabad neighborhood was modeled in 3D using GIS data from Tehran's District 6. Two scenarios were defined for comparison: Scenario 1, representing current conditions, and Scenario 2, reflecting approved development plans based on official building density (BD) and FAR regulations. Six representative blocks were selected to capture variations in form and orientation. Shapefiles, block footprints, and height data were imported into Rhino-Grasshopper to construct parametric models. Site coverage and FAR were calculated from GIS geometry, providing a quantitative basis for assessing morphological change and solar performance.

Simulation and Optimization

A. Solar Radiation and Daylighting Analysis

The solar and daylighting evaluation was structured in three analytical steps to operationalize the indicators introduced earlier (SR, S_H, SVF). Using Ladybug and Honeybee within Rhino–Grasshopper, annual and seasonal simulations were performed to quantify:

- Solar Radiation (SR): Annual cumulative solar radiation (kWh) was simulated for façades and open surfaces using grid-based sampling resolutions of 5 m (macro), 2 m (meso), and

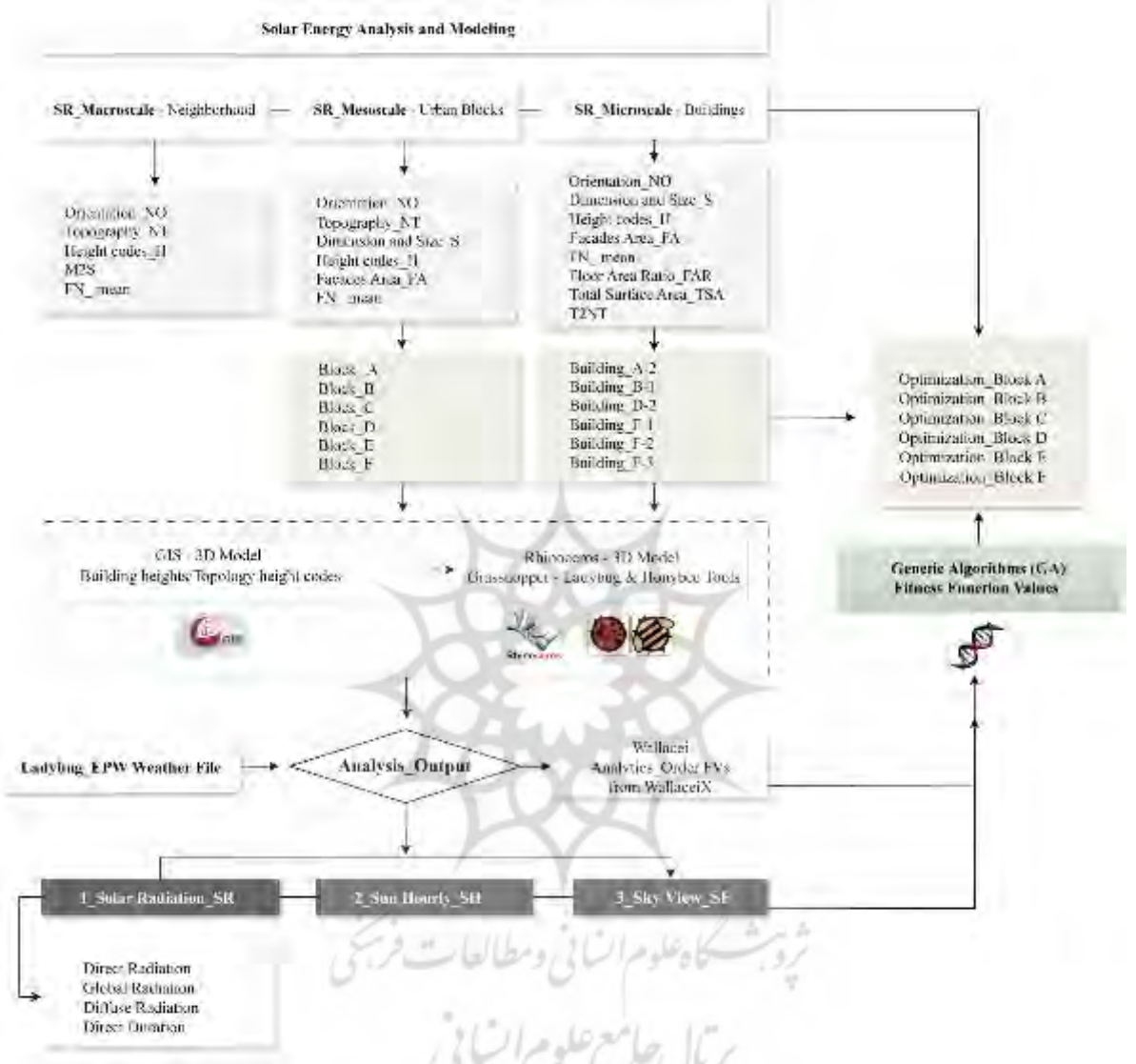

Fig. 5: Toolchain for multi-scale solar analysis and optimization. ArcGIS (3D blocks, indicators) → Rhino/Grasshopper + Ladybug/Honeybee (SR, S_H, SVF) → GA (optimization).

0.5 m (micro). The outputs quantify the total energy received and reveal shading effects from morphological density and building height.

- Sunlight Duration (S_H): Hourly radiation data were post-processed to calculate cumulative sunlight exposure (hours/year) for each surface. This step captured temporal variations in solar access and compared the performance of existing and approved development scenarios.

- Sky View Factor (SVF): Computed through Radiance hemispherical analysis to determine the visible portion of the sky dome for each grid point. The results were used to assess openness ratios and daylight obstruction within courtyards, streets, and semi-private spaces.

B. Optimization of Urban Blocks (Mesoscale)

This phase aims to identify the most efficient configuration of residential blocks to maximize solar access while meeting the regulatory constraints on urban density. The algorithm, illustrated in Figure 6, integrates a Genetic Algorithm (GA) within Grasshopper to iteratively evolve block configurations defined by morphological variables. Each configuration was encoded as a real-valued chromosome and evaluated based on solar radiation (SR) performance simulated via Ladybug–Honeybee.

C. Genetic Algorithm Configuration

The optimization employed a Genetic Algorithm (GA)

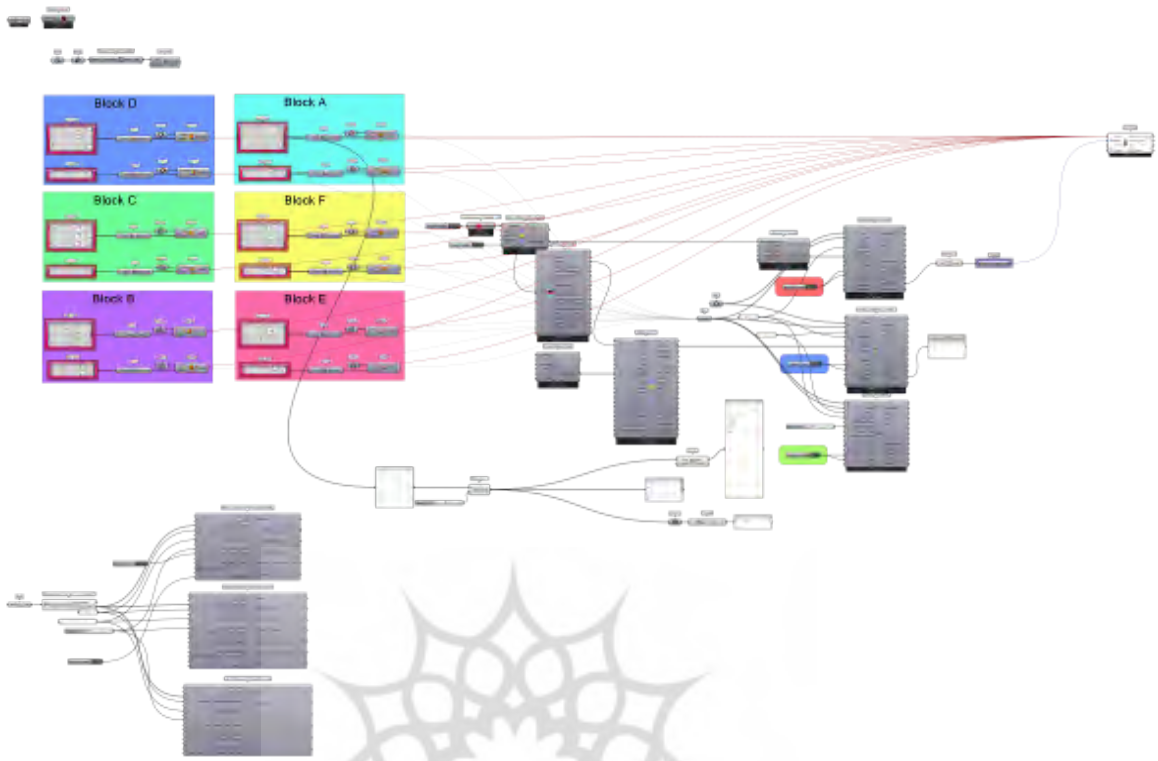

Fig. 6: Grasshopper-based genetic algorithm for block-scale SR optimization. Chromosome encoding, selection/crossover/mutation, constraint handling.

to evolve urban block configurations that maximize solar accessibility while satisfying regulatory constraints. Each chromosome encoded three morphological variables: building height (H), floor area ratio (FAR), and spacing ratio (S). The GA began with 10 constraint-compliant individuals and evolved over 20 generations. A tournament selection (size = 3), simulated binary crossover (rate = 0.8), and polynomial mutation (rate = 0.05) maintained diversity and prevented premature convergence. Constraints were enforced through a penalty-based correction ensuring legal height (≤ 27.5 m) and setback (≥ 3 m). The algorithm was executed three times to confirm repeatability, with convergence defined as $\Delta < 0.001$ or 20 generations. The procedure included the following stages:

I. Initialization: A population of feasible block configurations was randomly generated within legal limits.

II. Evaluation: Chromosomes were assessed using fitness functions based on solar access indicators (façade and open-space radiation).

III. Genetic Operations: Tournament selection favored individuals with higher fitness; crossover and mutation produced diverse offspring.

IV. Evolution: Generations iteratively improved, eliminating weaker solutions and reinforcing stronger ones.

V. Convergence: The process yielded a stable, balanced configuration that optimizes both density and solar accessibility.

The GA effectively simulated natural selection to refine urban form, demonstrating stable convergence and consistency across generations. The optimized block configurations balanced densification with equitable access to sunlight at the mesoscale.

As shown in Figure 7, the fitness value distribution (a) demonstrates clear improvement across generations, with later populations (red) outperforming initial ones (blue). The standard deviation curve (b) shows decreasing variability, indicating convergence toward stable solutions. The mean fitness trendline (c) rises steadily with a 23.15° slope, reflecting consistent optimization progress and reduced dispersion around the mean.

D. Equity Metrics and Objective Formulation

To complement the GA-based performance optimization, an explicit equity objective was incorporated to quantify the fairness of solar access distribution among residential buildings. This ensured that the optimization framework not only maximized total solar gain but also minimized disparities in sunlight and sky exposure across blocks. Equity, as expressed in Equation (1), was evaluated using the Gini coefficient (G), calculated for three solar-related indicators, solar radiation (SR), sunlight hours (S_H), and sky view factor (SVF), across all buildings within the six representative blocks:

$$G(\boldsymbol{v}) = \frac{\sum_{j=1}^{n}\sum_{i=1}^{n}|v_i - v_j|}{2n^2\mu} \qquad \text{Equation (1)}$$

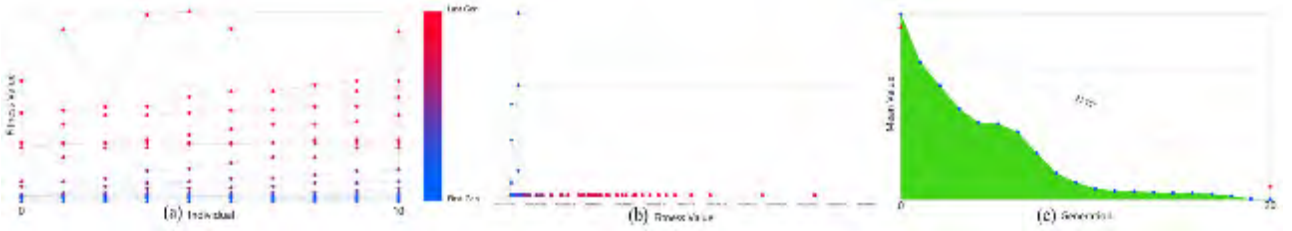

Fig. 7: GA performance trends (mesoscale). (a) Fitness values by generation; (b) standard deviation (convergence stability); (c) mean trendline across generations. Notes: pop=10, gen=20.

where is the indicator value of building i, and is its mean across the population. A higher number indicates greater inequality. For optimization purposes, an equity score was defined as E = 1 - G, where higher values indicate a fairer distribution. Following the equity formulation, the optimization problem was parameterized as follows:

- Decision Variables: The variable vector X encodes block-level morphology, including building heights within code limits, bulk distribution relative to open spaces, and geometric ratios constrained by urban regulations.

- Objectives: The multi-objective optimization, as formulated in Equation (2), sought to maximize solar performance and equity simultaneously and can be expressed as:

$$F(x)_{max} = \left[(G_{(SVF)} - G_{(SH)}), (1 - G_{SR}), (1 - \mu_{SR}), \mu_{(SH)}, \mu_{(SVF)}, 1\right]$$

Equation (2)

subject to

$$FAR_b(x) \leq FAR_b^{max}, \quad \forall b \qquad H_p^{min} \leq H_p(x) \leq H_p^{max}, \quad \forall p$$

Ensuring that setbacks, coverage ratios, and H\W proportions comply with local planning codes. All objectives were min–max normalized to the range [0, 1] before non-dominated sorting. The NSGA-II algorithm (population = 10, generations = 20) with simulated binary crossover and polynomial mutation identified Pareto-optimal solutions balancing solar performance and equity. The knee-point solution was determined using the Kneedle algorithm, which represents the optimal trade-off between solar efficiency and equitable access.

E. Uncertainty and Robustness Evaluation

To ensure the methodological robustness and reproducibility of the simulation–optimization framework, uncertainty analyses were performed on both climatic inputs and model parameters. Variations of ±5% in solar radiation intensity and ±3% in sunlight duration were introduced, consistent with long-term fluctuations in the Tehran IWEC dataset. Radiance parameters, ambient bounces, divisions, and resolution were cross-validated using a supplementary test with a doubled grid density. Across all tests, deviations in key solar indicators (SR, S_H, and SVF) remained below ±6%, confirming numerical stability. Additionally, the optimization module was executed in three independent GA runs to assess stochastic repeatability. The final fitness values exhibited a coefficient of variation (CV) of 0.037, with convergence achieved in all runs before the 18th generation. These results verify that both simulation and optimization procedures are stable and repeatable, providing a reliable foundation for the performance results discussed in the following section.

RESULTS AND DISCUSSION

At the macroscale, the analysis examined how large-scale morphological changes affect solar access in the neighborhood. Two scenarios were modeled: the existing condition (Scenario 1) and the approved densification plan (Scenario 2). In Scenario 1, total solar radiation reached 1.68×10^7 kWh, with a mean irradiance of about 1.2 kWh·yr, while in Scenario 2 it declined to 1.14×10^7 kWh, a 32% reduction due to increased height and density, which intensified shading and limited solar penetration. Figure 8(a) illustrates the spatial distribution of irradiance and sunlight duration for both scenarios.

As shown in Figure 8(b), densification in the approved scenario increases shading and reduces solar radiation (SR) and sunlight duration (S_H) at lower levels, concentrating exposure on upper façades. The spatial maps reveal a clear shift in solar access patterns.

At the mesoscale, as shown in Table 7, densification significantly modifies both solar performance and morphological characteristics across blocks. Scenario 2 shows higher total solar radiation (SR ≈ 1.48×10^8 kWh) and longer sunlight duration (S_H ≈ 2.97×10^8 h) due to expanded vertical surfaces, while the average sky view factor (SVF) declines from 37.5% to 30.7%, reflecting reduced openness and increased mutual shading. Overall, densification enhances total energy capture but limits daylight availability at lower levels, underscoring the need for balanced height regulation to maintain equitable solar access.

At the microscale, exterior illuminance was measured at

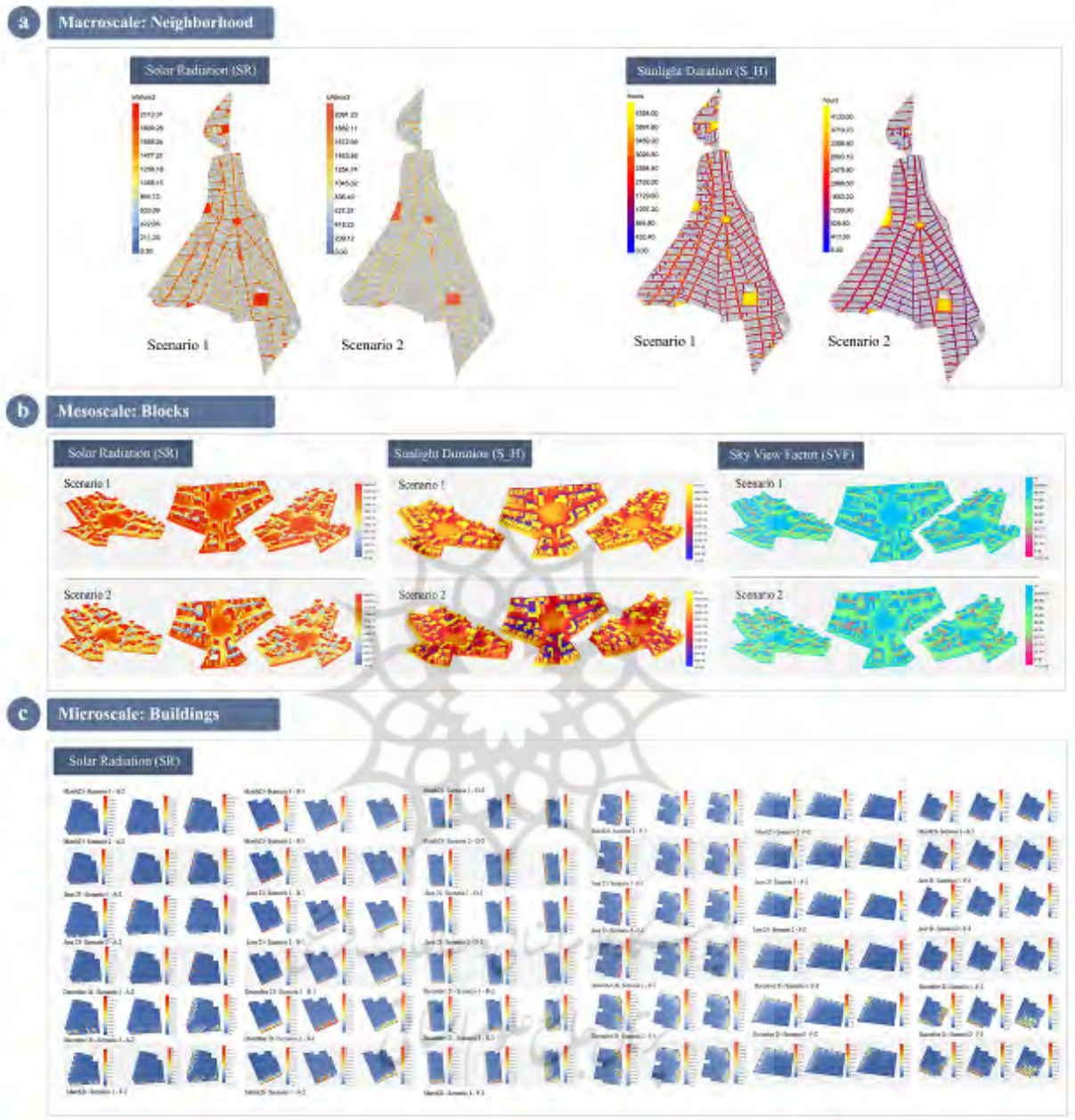

Fig. 8: (a) Macroscale, (b) Mesoscale, and (c) Microscale analyses of SR (kWh/yr), S_H (h/yr), and SVF (%) across development scenarios.

three time intervals—9:00, 12:00, and 15:00—to capture daily variations across different orientations and façade configurations, as summarized in Table 8.

As shown in Table 8 and Figure 8(c), façade illuminance and sunlight penetration vary significantly between scenarios and building types. Buildings with larger openings and favorable orientations (A-2, B-1, F-1, F-2, and F-3) receive greater daylight depth in spring and summer, while densified layouts in Scenario 2 reduce illuminance, especially during winter. These results indicate that increased compactness and height diminish daylight quality and equity of solar access within residential buildings.

Optimized Scenario and Equity Evaluation (Scenario 3)

In the optimized scenario (Scenario 3), block density and building heights were refined to achieve the most efficient solar access configuration for the Yousefabad neighborhood.

As shown in Figure 9, the optimized model provides more balanced solar access across all blocks than Scenarios 1 and 2. Interior and semi-private spaces benefit most, as reduced

Table 7: Mesoscale quantitative comparison of SR, S_H, SVF, and heights. Blocks A–F: SR (kWh), S_H (h), SVF (%), height (m)

Scenario 1		Block A	Block B	Block C	Block D	Block E	Block F	Blocks	Blocks	Urban	Total
Radiation (Kwh)		1.69E+07	1.86E+07	1.40E+07	9.04E+06	9.14E+06	1.68E+07	8.44E+07	1.93E+07	3.40E+07	1.38E+08
Sunlight (Hours)		3.43E+07	3.91E+07	2.98E+07	1.91E+07	1.94E+07	3.50E+07	1.77E+08	3.34E+07	5.72E+07	2.67E+08
Sky View (%)		36.69	34.35	33.75	41.43	38.66	32.83	35.48	22.49	69.94	37.47
Radiation (kWh/m·year)		1.64E+05	1.12E+05	1.52E+05	1.33E+05	1.40E+05	6.19E+04	7.62E+05			
Number of Buildings	Far from Square	8	10	6	6	5	23	58			
	Near Square	2	3	1	1	1	2	10			
Far from (m) Square	Average Height	9.97	13.42	11.92	9.66	10.55	10.74	11.04			
	Max Height	18.00	21.19	0.87	15.00	15.00	27.24	27.24			
	Min Height	3.41	6.00	21.00	4.00	6.00	3.00	3.00			
Near Square ((m	Average Height	11.47	10.65	20.91	10.00	12.66	12.01	12.95			
	Max Height	24.29	18.00	20.91	10.00	12.66	13.00	24.29			
	Min Height	6.00	3.00	20.91	10.00	12.66	7.14	3.00			
Far from Square	Total Height	79.76	134.20	71.52	57.96	52.75	247.02	643.21			
Near Square	Total Height	22.94	31.95	20.91	10.00	12.66	24.02	122.48			
Scenario 2		Block A	Block B	Block C	Block D	Block E	Block F	Blocks	Blocks	Urban	Total
Radiation (Kwh)		2.11E+07	2.20E+07	1.52E+07	1.31E+07	1.07E+07	2.08E+07	1.03E+08	1.47E+07	3.01E+07	1.48E+08
Sunlight (Hours)		4.53E+07	4.81E+07	3.24E+07	2.88E+07	2.28E+07	4.46E+07	2.22E+08	2.56E+07	4.97E+07	2.97E+08
Sky View (%)		29.18	29.81	31.50	34.00	32.68	24.96	29.43	17.08	61.37	30.67
Radiation (kWh/m·year)		9.32E+04	8.35E+04	1.12E+05	7.65E+04	1.11E+05	3.85E+04	5.15E+05			
Number of Buildings	Far from Square	8	10	6	6	5	23	58			
	Near Square	2	3	1	1	1	2	10			
Far from (Square (m	Average Height	22.75	20.23	19.08	24.00	16.69	21.75	20.75			
	Max Height	29.69	29.57	29.43	29.45	29.48	29.83	29.83			
	Min Height	10.44	12.61	10.91	15.85	10.64	12.02	10.44			
Near Square ((m	Average Height	22.12	20.56	20.91	27.51	12.66	19.94	20.62			
	Max Height	29.65	27.99	20.91	27.51	12.66	13.00	27.99			
	Min Height	16.68	12.13	20.91	27.51	12.66	26.21	12.13			
Far from Square	Total Height	182.00	202.30	114.48	144.00	83.45	500.25	1226.48			
Near Square	Total Height	44.24	61.68	20.91	27.51	12.66	39.88	206.88			

Table 8: Simulated façade illuminance (lux) at microscale. Three reference days (21 March, 21 June, 21 December) for Scenarios 1 and 2. Notes: exterior incident illuminance.

			Building ID					
Scenario 1		Time	A-2	B-1	D-2	F-1	F-2	F-3
Moderate	March - 21	9:00	833.50	1747.92	1247.00	2353.91	364.36	2277.07
	March - 21	12:00	1417.54	2051.88	2165.87	828.82	528.92	2680.21
	March - 21	15:00	1445.30	464.11	2759.78	556.53	918.08	1677.90
Warmest	June - 21	9:00	550.32	1462.34	960.83	2749.77	504.78	2468.20
	June - 21	12:00	948.44	911.71	1510.50	798.71	596.73	1591.02
	June - 21	15:00	1797.32	436.92	2730.09	631.25	1468.98	1229.15
Coldest	December - 21	9:00	642.55	359.65	944.26	1043.30	222.95	1528.75
	December - 21	12:00	1170.13	2158.33	2075.68	564.91	358.67	2428.94
	December - 21	15:00	754.39	436.03	1280.68	301.08	399.74	1137.66
			Building ID					
Scenario 2		Time	A-2	B-1	D-2	F-1	F-2	F-3
Moderate	March - 21	9:00	724.49	1535.38	1242.64	2289.64	349.54	2147.67
	March - 21	12:00	1328.22	1813.47	2148.29	801.67	533.06	2613.10
	March - 21	15:00	1396.01	393.90	2799.98	798.79	910.05	1634.59
Warmest	June - 21	9:00	477.63	1340.79	958.83	2664.39	459.35	2384.61
	June - 21	12:00	905.75	817.97	1471.70	753.55	574.63	1554.03
	June - 21	15:00	1771.16	407.91	2551.39	574.92	1437.49	1223.11
Coldest	December - 21	9:00	254.47	233.97	937.22	996.18	215.19	1007.73
	December - 21	12:00	916.24	1162.48	2061.26	526.00	373.08	2352.34
	December - 21	15:00	706.15	378.41	1292.88	262.97	403.79	1110.92

Fig. 9: Scenario 3 (optimized): annual radiation distribution. More uniform SR and improved exposure in interior/semi-private spaces.

shading improves exposure to natural light. These results demonstrate that optimized morphological design can offset the negative effects of densification while maintaining sufficient daylight throughout the neighborhood. Table 9 presents block-level results and building height distribution, confirming that the optimized configuration offers superior solar performance and more equitable daylight accessibility than the previous scenarios.

As shown in Table 9, the optimized scenario records a cumulative solar radiation of 1.36×10^8 kWh and an average SVF of nearly 40%, indicating a more balanced solar distribution. The adjusted height configuration reduces overshadowing while maintaining morphological balance, enhancing daylight availability, and ensuring equitable solar access across the urban fabric.

Equity Outcomes and Pareto Front Analysis

This section evaluates efficiency, equity, and the trade-offs between them in solar access performance across different morphological configurations. The analysis employs Pareto fronts generated by the NSGA-II algorithm, which simultaneously optimize the mean solar indicators —solar radiation (SR), sunlight hours (S_H), and sky view factor (SVF) —alongside their Gini-based equity measures (G_SR20, G_S_H21, G_SVF22). Table 11 presents the mean values and Gini coefficients for the three key solar indicators across the evaluated scenarios.

As summarized in Table 10, the optimized configuration (Scenario 3) yields the lowest Gini coefficients across all indicators (G_SR = 0.094, G_S_H = 0.089, G_SVF = 0.084), reflecting an overall 16–20% improvement in equity compared to the densified condition (Scenario 2). Despite a moderate reduction in mean SR, both sunlight duration and sky view factor improve, indicating a more balanced and equitable solar distribution. Figure 14 illustrates these trade-offs, showing how

Table 9: Scenario 3 (optimized) block-level indicators. SR (kWh), S_H (h), SVF (%), building height (m)

Scenario 3_Optimal Model		Block A	Block B	Block C	Block D	Block E	Block F	Blocks	Blocks	Urban	Total
(Radiation (Kwh		1.76E+07	1.77E+07	1.26E+07	1.02E+07	8.71E+06	1.66E+07	8.34E+07	1.94E+07	3.33E+07	1.36E+08
Sunlight (Hours)		3.80E+07	3.85E+07	2.73E+07	2.24E+07	1.94E+07	3.53E+07	1.81E+08	3.35E+07	5.52E+07	2.70E+08
(%) Sky View		40.08	40.80	36.27	40.18	43.09	38.94	39.23	22.72	69.08	39.76
Radiation (kWh/(m·year		1.57E+05	1.36E+05	1.51E+05	1.21E+05	1.46E+05	6.78E+04	7.79E+05			
Number of Buildings	Far from Square	8	10	6	6	5	23	58			
	Near Square	2	3	1	1	1	2	10			
Far from Square (m)	Average Height	10.06	8.75	10.50	10.50	8.40	9.28	9.58			
	Max Height	14.00	14.00	14.00	14.00	10.50	14.00	14.00			
	Min Height	7.00	7.00	3.50	3.50	7.00	3.50	3.50			
Near Square (m)	Average Height	15.75	14.00	21.00	21.00	17.50	15.75	17.50			
	Max Height	17.50	17.50	21.00	21.00	17.50	17.50	21.00			
	Min Height	14.00	7.00	21.00	21.00	17.50	14.00	7.00			
Far from Square	Total Height	80.50	87.50	63.00	63.00	42.00	213.50	549.50			
Near Square	Total Height	31.50	42.00	21.00	21.00	17.50	31.50	164.50			

Table 10. Means and Gini coefficients for SR, S_H, and SVF by scenario. Scenario 1/2/3: Mean values and G_SR, G_S_H, G_SVF (dimensionless).

	SR		S_H		SVF	
Scenario	**Mean SR** (kWh)	**G_SR**	**Mean S_H** (Hours)	**G S_H**	**Mean SVF** (%)	**G_SVF**
Scenario 1 (Current)	1.45×10^7	0.112	3.36×10^7	0.098	36.55	0.090
Scenario 2 (Approved)	1.68×10^7	0.145	3.80×10^7	0.121	30.34	0.110
Scenario 3 (Optimized)	1.39×10^7	0.094	3.38×10^7	0.089	39.05	0.084

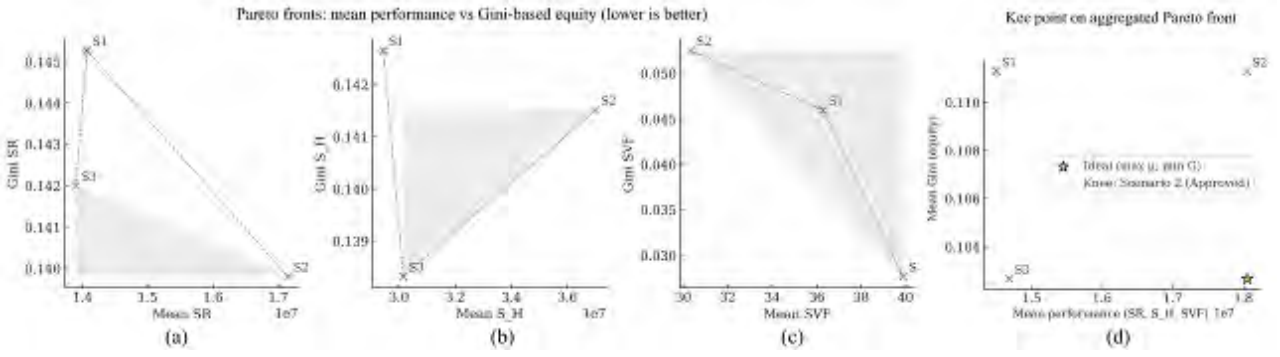

Fig. 10: Pareto front analysis of efficiency–equity trade-offs in solar performance. (a–c) Mean performance versus Gini-based equity for SR, S_H, and SVF (lower Gini indicates higher equity). (d) Aggregated Pareto front showing the knee point

variations in urban form influence both overall performance and the fairness of solar access distribution.

As shown in Figure 10, the Pareto fronts demonstrate that the optimized scenario (S3) achieves the best balance between solar performance and equity, shifting toward higher efficiency and lower inequality across SR, S_H, and SVF. The aggregated front identifies Scenario 2 as the knee point, indicating that moderate densification yields an effective trade-off between solar efficiency and spatial fairness.

Integrated Evaluation of the Three Scenarios

A comparative evaluation of the three scenarios demonstrates how variations in urban form influence both solar performance and spatial equity in Yousefabad. The analysis integrates building height, solar radiation (SR), sunlight duration (S_H), and sky view factor (SVF) to assess the overall efficiency and fairness of each morphological configuration.

As shown in Table 11 and Figure 11, while the approved densification (Scenario 2) yields the highest solar radiation and sunlight hours, its pronounced reduction in sky view factor (SVF) signals spatial enclosure and diminished pedestrian-scale daylight. In contrast, the optimized configuration (Scenario 3) recalibrates this imbalance, reducing average height while maintaining comparable SR and S_H, resulting in superior daylight quality, spatial openness, and livability. The integrated trends confirm that solar efficiency alone cannot indicate environmental success; rather, morphological equilibrium between height, openness, and solar distribution is the critical determinant of resilient urban form.

Equity-Based Assessment of Solar Access

Beyond the scenario-based comparison presented earlier, this section focuses on spatial equity —how evenly solar benefits are distributed across different blocks and within each block's internal zones. To quantify this aspect, three core indicators were evaluated alongside their Gini coefficients (G_SR, G_S_H, and G_SVF), which represent the degree of inequality in solar access, as detailed in Table 12.

As shown in Table 12, the Approved Densification scenario achieves the highest mean SR and S_H values due to greater façade exposure, but at the cost of equity, as Gini indices rise to 0.331, 0.298, and 0.265 for SR, S_H, and SVF, respectively. The Optimized scenario maintains sufficient solar performance while reducing inequality by 29%, 31%, and 42%, respectively.

Height-Code Translation

To translate the optimized results into actionable design guidance, block-level height codes were derived from the final morphological dataset. These codes establish minimum, maximum, and step-height values that ensure both adequate solar performance and equitable exposure. The recommended configurations correspond to the most stable SVF range (≈ 38–42 %) and consistent sunlight duration across the inner and outer block segments, as detailed in Table 13.

Each block was subdivided by its median distance (d*) from the geometric center, defining Inner and Outer zones. As shown

Table 11: Integrated scenario comparison. Avg. Height (m), Total SR (kWh), S_H (h), Mean SVF (%), main outcome per scenario.

Scenario	Avg. Height (m)	Total SR (kWh)	Sunlight Hours (SH)	Mean SVF (%)	Main Outcome
Scenario 1 (Current Condition)	11.95	1.38×10^8	2.67×10^8	37.5	Balanced daylight, moderate density
Scenario 2 (Approved Densification)	20.7	1.48×10^8	2.97×10^8	30.7	Higher SR but reduced openness
Scenario 3 (Optimized Model)	13.55	1.36×10^8	2.70×10^8	39.8	Improved equity and livability

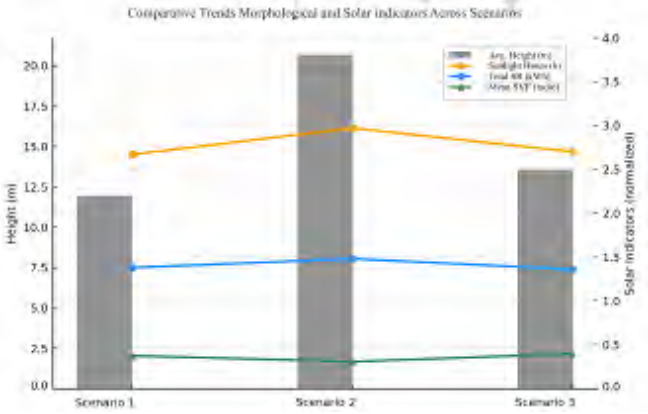

Fig. 11: Integrated comparison of morphological and solar indicators.Scenario 1-3, for Avg. Height (m), Total SR (kWh), S_H (h), and SVF (%).

Table 12: Equity-focused block-level comparison across scenarios. Notes: normalized to façade area.

Scenario	Mean SR (kWh·yr)	G_SR	Mean S_H (h/yr)	G_S_H	Mean SVF (%)	G_SVF
Scenario 1 (Current Condition)	1.23×10^3	0.268	3.05×10^7	0.241	35.48	0.182
Scenario 2 (Approved Densification)	1.42×10^3	0.331	3.41×10^7	0.298	29.43	0.265
Scenario 3 (Optimized Model)	1.27×10^3	0.192	3.17×10^7	0.205	39.23	0.153

Table 13: Inner/outer zone statistics and derived block-level height-code ranges (min–max–step)m() of scenarios.

Scenario 1 (Current Condition)							
Block	Median d* (m)	Inner (≤ d*) – Avg Height (m)	Outer (> d*) – Avg Height (m)	Inner SR (kWh)	Outer SR (kWh)	Inner SVF (%)	Outer SVF (%)
A	75	9.8	11.1	1.64×10^5	1.51×10^5	36.7	33.4
B	85	13.4	14.1	1.12×10^5	1.05×10^5	34.3	32.9
C	95	11.9	13.5	1.52×10^5	1.43×10^5	33.8	31.7
D	110	9.6	10.8	1.33×10^5	1.26×10^5	41.4	38.2
E	120	10.6	11.4	1.40×10^5	1.33×10^5	38.7	36.1
F	130	10.7	11.2	6.19×10^4	5.84×10^4	32.8	30.9
Scenario 2 (Approved Densification)							
Block	Median d* (m)	Inner (≤ d*) – Avg Height (m)	Outer (> d*) – Avg Height (m)	Inner SR (kWh)	Outer SR (kWh)	Inner SVF (%)	Outer SVF (%)
A	75	22.1	20.6	9.32×10^4	8.95×10^4	29.2	28.1
B	85	20.2	19.9	8.35×10^4	8.10×10^4	29.8	28.7
C	95	19.1	18.4	1.12×10^5	1.07×10^5	31.5	29.9
D	110	24.0	22.7	$10^4\times7.65$	7.20×10^4	34.0	31.6
E	120	16.7	15.9	1.11×10^5	1.06×10^5	32.7	30.4
F	130	21.7	20.6	3.85×10^4	3.70×10^4	24.9	23.6
Scenario 3 (Optimized Model)							
Block	Median d* (m)	Inner (≤ d*) – Avg Height (m)	Outer (> d*) – Avg Height (m)	Min Height (m)	Max Height (m)	Step (m)	Inner SR (kWh)	Outer SR (kWh)	Inner SVF (%)	Outer SVF (%)
A	75	10.1	9.6	9.5	11.0	0.6	1.57×10^5	1.48×10^5	40.1	37.8
B	85	8.8	8.5	9.0	10.8	0.5	1.36×10^5	1.29×10^5	40.8	39.1
C	95	10.5	10.3	9.4	10.5	0.4	1.51×10^5	1.42×10^5	36.3	34.2
D	110	10.5	9.9	8.8	10.2	0.7	1.21×10^5	1.16×10^5	40.2	38.5
E	120	8.4	8.1	7.8	9.2	0.5	1.46×10^5	1.38×10^5	43.1	41.3
F	130	9.3	8.8	8.0	9.8	0.6	6.78×10^4	6.45×10^4	38.9	36.5

in Table 13, densification reduces both SR and SVF, while the optimized scenario restores balance (SR ≈ 1.5×10^5 kWh; SVF ≈ 38–43 %). The resulting height-code ranges (8–11 m) maintain proportional solar access and equity across blocks.

Urban Design Guideline Based on Height-Code and Solar Equity Evaluation

A. Macro Scale – Neighborhood

Objective: To guide urban form toward balanced density, solar access, and environmental equity at the neighborhood scale.

Design Guideline:

-G1.A: Regulate average building height according to the median distance from the block center (d*) to maintain a balanced distribution of solar radiation and sky exposure.

-G2.A: Inner zones (≤ d*) should maintain heights between 8 m and 11 m (approximately two to three stories) to preserve daylight access and courtyard illumination.

-G3.A: Outer zones (> d*) may reach 14–16 m (about four stories), provided that the sky view factor (SVF) remains within 38–42 %.

-G4.A: Any redevelopment process should ensure that the reduction in solar access equity (SR or SVF) does not exceed 10 % compared to the baseline condition.

-G5.A: Zoning and redevelopment plans should integrate height-code layers as regulatory overlays to support gradual, equitable densification across compact neighborhoods.

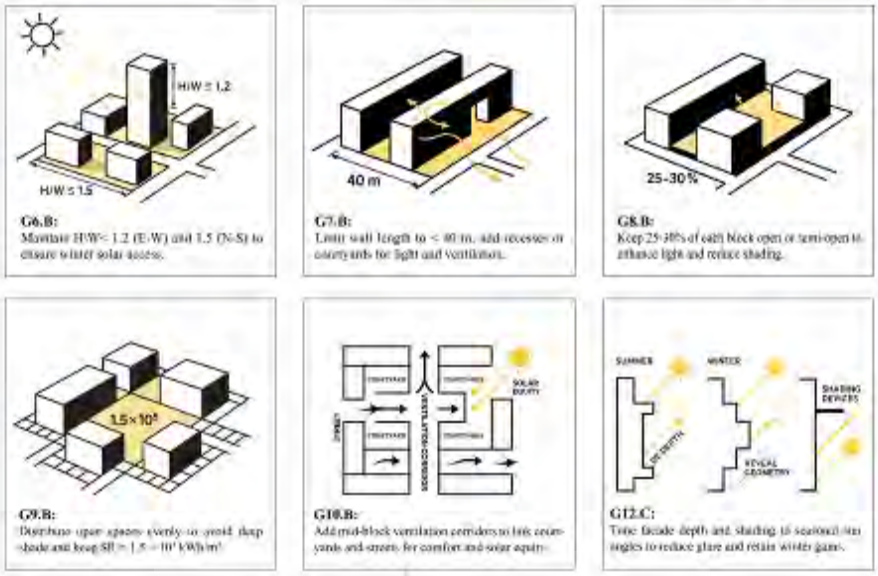

Fig. 12: Solar-oriented urban design guidelines.

B. Meso Scale – Block and Intermediate Morphology

Objective: To sustain daylight quality, ventilation potential, and balanced density within urban blocks. Design Guideline:

- G6.B: Maintain height-to-width (H/W) ratios below 1.2 for east–west corridors and below 1.5 for north–south streets to ensure winter solar penetration.
- G7.B: Avoid continuous building walls exceeding 40 m in length without recesses, courtyards, or breaks; periodic voids enhance daylight distribution and air circulation.
- G8.B: Preserve 25–30 % of each block's total area as open or semi-open space. These voids act as solar receivers, redistributing reflected light and mitigating overshadowing.
- G9.B: In compact blocks, distribute open spaces evenly to prevent deep-shade zones, maintaining mean solar radiation values around 1.5×10^5 kWh in central areas.
- G10.B: Introduce mid-block ventilation corridors to connect courtyards and streets, supporting both thermal comfort and solar equity.

C.Micro Scale – Building and Architectural Components

Objective: To ensure fair solar access, daylight quality, and thermal comfort at the building scale. Design Guideline:

-G11.C: Internal courtyards should maintain a width-to-height ratio (W/H ≥ 1.5), guaranteeing at least four hours of direct sunlight on winter days.

-G12.C: Adjust façade depth, reveal geometry, and shading devices to align with seasonal solar angles, minimizing glare while retaining passive winter gains.

-G13.C: Apply solar-equity thresholds to evaluate design fairness:

-GSR ≤ 0.20 (Global Solar Radiation equity)

-GSH ≤ 0.22 (Sunlight Hours equity)

-GSVF ≤ 0.18 (Sky View Factor equity)

-G14.C: When simulated values exceed these thresholds, apply corrective measures such as minor height reduction or increased open-space ratio.

-G15.C: Ensure that façade and window design support adequate daylight penetration to interior spaces without casting excessive shadows on adjacent units.

Discussion

This study provides evidence that solar equity can be achieved through adaptive morphological regulation rather than uniform densification. The results indicate that the spatial organization of height, rather than its absolute magnitude, governs the distribution of solar benefits within compact neighborhoods. The optimized configuration confirms that the most effective urban form is not defined by maximum solar gain, but by a balanced relationship between density, height, and spatial openness. This highlights the urban equity dimension of solar design, ensuring fair sunlight distribution among adjacent plots. These findings reinforce the idea that equitable access to sunlight is not only a technical outcome of energy modeling but also a spatial and social condition of urban form.

By integrating quantitative solar indicators with equity-based evaluation, the research reframes solar rights as a performance criterion that can be embedded directly into planning regulations. This approach expands the role of environmental simulation from a diagnostic tool to a regulatory instrument, linking design performance with spatial justice. Beyond its local application in Yousefabad, the framework demonstrates broader methodological relevance. It shows how multi-scalar analysis, spanning neighborhood, block, and building levels, can reveal systemic patterns of inequity in dense urban forms.

The integration of genetic optimization and equity assessment provides a replicable workflow that can inform urban policies in other rapidly densifying contexts. More broadly, this study contributes to the ongoing discourse on sustainable urban morphology, emphasizing that the success of densification depends not only on energy efficiency but also on the equitable distribution of environmental benefits. Future research could extend this framework by incorporating dynamic climatic variables, seasonal adaptability, and socio-economic dimensions of solar access to advance evidence-based, justice-oriented urban design.

CONCLUSION

This study advances the understanding of how urban morphology can be designed to support both solar efficiency and spatial equity. The results suggest that the distribution of building heights and open spaces, rather than the total built volume alone, determines the fairness of solar access in dense neighborhoods. By operationalizing solar rights as quantifiable design criteria, the research reframes sunlight as an environmental entitlement that can be evaluated and regulated through measurable indicators. This conceptual shift connects environmental performance to the broader discourse on urban equity and spatial justice, positioning solar access as a shared urban resource rather than a by-product of form.

Methodologically, integrating multi-scalar simulation and equity-based optimization establishes a replicable framework for linking morphological parameters to social and environmental outcomes. The approach demonstrates how design decisions at one scale influence performance at others, revealing the systemic nature of solar inequality in compact urban forms. Beyond the Yousefabad context, the framework provides a transferable foundation for developing context-sensitive height codes and equitable densification policies. Future studies could extend this work by incorporating seasonal variability, adaptive façade strategies, and socio-economic data to deepen the understanding of how environmental justice principles can guide sustainable urban growth.

ENDNOTES

1. NO: Neighborhood Orientation (Northwest, Southeast, North-East, Southwest)
2. Northwest
3. Southeast
4. North-East
5. Southwest
6. FN: Form of the Neighborhood
7. MD: Macroscale Density
8. Neighborhood Typology: Classification based on spatial configuration
9. BZ_mean: Average block size
10. M2S: Mass to Space Ratio
11. H_mean: Average Height
12. FN_mean: Average Floor Number
13. FAR: Floor Area Ratio
14. GOP: Gross Open Space Pattern
15. Linear-central
16. Linear
17. Open Space in the Center
18. Open Space in the South
19. Active façade: Sun-receiving building side with windows or openings admitting daylight
20. Gini coefficient of Solar Radiation: measures how evenly solar radiation is distributed across the study area.
21. Gini coefficient of Sunlight Hours: measures the equity of sunlight duration among urban blocks.
22. Gini coefficient of Sky View Factor: indicates how equitably sky openness is distributed across urban spaces.

AUTHOR CONTRIBUTIONS

N. Mosalmanfarkoosh conceived and designed the research, developed the methodology, conducted the analysis and investigation, and prepared the original draft of the manuscript.

H. Pendar supervised the research process, validated the results, and contributed to manuscript revision.

P. Alipour Kouhi provided advisory support, assisted with data curation, and contributed to manuscript editing.

Niu. Mosalmanfarkoosh contributed to visualization, data interpretation, and manuscript review.

ACKNOWLEDGEMENT

This paper is derived from the author's master's thesis in Urban Design at the Art University of Tehran. The authors thank the Department of Urban Design, Faculty of Architecture and Urban Planning, for their academic support.

CONFLICT OF INTERESt

The authors declare no potential conflict of interest regarding the publication of this work. In addition, the ethical issues, including plagiarism, informed consent, misconduct, data fabrication and/or falsification, double publication and/or submission, and redundancy, have been fully witnessed by the author.

REFERENCES

Amado, M. P., Poggi, F., & Amado, A. R. (2016). Energy-efficient city: A model for urban planning. Sustainable Cities and Society, 26, 476–485. https://doi.org/10.1016/j.scs.2016.04.011

Bentley, I., Alcock, A., Murrain, P., McGlynn, S., & Smith, G. (1985). Responsive environments: A manual for designers. Architectural Press.

Cheng, V., Steemers, K., Montavon, M., & Compagnon, R. (2006, 1 September). Urban form, density, and solar potential. In Proceedings of the 23rd Conference on Passive and Low Energy Architecture (PLEA 2006) (Vol. 6). Geneva, Switzerland: EPFL. Retrieved from https://infoscience.epfl.ch/record/84787/files/PLEA2006_UrbanFormDensityAndSolarPotential.pdf

4. De Luca, F., Dogan, T., & Sepúlveda, A. (2021). Reverse solar envelope method: A new building form-finding method that can take regulatory frameworks into account. Automation in Construction, 123, 103518. https://doi.org/10.1016/j.autcon.2020.103518

Doherty, M., Nakanishi, H., Bai, X., & Myers, J. (2009, October 16–18). Relationships between form, morphology, density, and energy in urban environments. In Proceedings of the International Conference on Human Ecology (pp. 1–28). The Society for Human Ecology.

Elaouzy, Y. (2025). Enhancing urban planning for sustainable and solar-optimized neighborhoods: A case study from Morocco. Solar Energy, 244, 113732. https://doi.org/10.1016/j.solener.2025.113732

Ferrando, M., Causone, F., Hong, T., & Chen, Y. (2020). Urban building energy modeling (UBEM) tools: A state-of-the-art review of bottom-up physics-based approaches. Sustainable Cities and Society, 62, 102408. https://doi.org/10.1016/j.scs.2020.102408

Freitas, S., Catita, C., Redweik, P., & Brito, M. C. (2015). Modelling solar potential in the urban environment: State-of-the-art review. Renewable and Sustainable Energy Reviews, 41, 915–931. https://doi.org/10.1016/j.rser.2014.08.060

Geng, X., Xie, D., & Gou, Z. (2024). Optimizing urban block morphologies for net-zero energy cities: Exploring photovoltaic potential and urban design prototypes. Building Simulation, 17(4), 607–624. https://doi.org/10.1007/s12273-024-1104-y

Kanters, J., & Horvat, M. (2012). Solar energy as a design parameter in urban planning. Energy Procedia, 30, 1143–1152. https://doi.org/10.1016/j.egypro.2012.11.127

Liu, K., Xu, X., Zhang, R., Kong, L., Wang, W., & Deng, W. (2023). Impact of urban form on building energy consumption and solar energy potential: A case study of residential blocks in Jianhu, China. Energy and Buildings, 280, 112727. https://doi.org/10.1016/j.enbuild.2022.112727

Lobaccaro, G., Frontini, F., Masera, G., & Poli, T. (2012). SolarPW: A new solar design tool to exploit solar potential in existing urban areas. Energy Procedia, 30, 1173–1183. https://doi.org/10.1016/j.egypro.2012.11.130

Lobaccaro, G., Lisowska, M. M., Saretta, E., Bonomo, P., & Frontini, F. (2019). A methodological analysis approach to assess solar energy potential at the neighborhood scale. Energies, 12(18), 3554. https://doi.org/10.3390/en12183554

Mirzabeigi, S., & Razkenari, M. (2022). Design optimization of urban typologies: A framework for evaluating building energy performance and outdoor thermal comfort. Sustainable Cities and Society, 76, 103515. https://doi.org/10.1016/j.scs.2021.103515

Moonen, P., Defraeye, T., Dorer, V., Blocken, B., & Carmeliet, J. (2012). Urban physics: Effect of the microclimate on comfort, health, and energy demand. Frontiers of Architectural Research, 1(3), 197–228. https://doi.org/10.1016/j.foar.2012.05.002

Morganti, M., Salvati, A., Roura, H. C., & Cecere, C. (2017). Urban morphology indicators for solar energy analysis. Energy Procedia, 134, 807–814. https://doi.org/10.1016/j.egypro.2017.09.533

Mosalmanfarkoosh, N. (2025). Urban Design Guideline Related to Physical Density Focusing on Solar Right of Residents – Case Study: Yousefabad Neighborhood, Tehran [Zenodo]. https://doi.org/10.5281/zenodo.17328781

Oh, M., Jang, K. M., & Kim, Y. C. (2021). Empirical analysis of building energy consumption and urban form in a large city: A case of Seoul, South Korea. Energy and Buildings, 245, 111046. https://doi.org/10.1016/j.enbuild.2021.111046

Okeil, A. (2010). A holistic approach to energy-efficient building forms. Energy and Buildings, 42(9), 1437–1444. https://doi.org/10.1016/j.enbuild.2010.03.013

Pakzad, E., & Salari, N. (2018). Measuring sustainability of urban blocks: The case of Dowlatabad, Kermanshah city. Cities, 75, 90–100. https://doi.org/10.1016/j.cities.2018.01.005

Poggi, F., & Amado, M. P. (2024). The spatial dimension of energy consumption in cities. Energy Policy, 187, 114023. https://doi.org/10.1016/j.enpol.2024.114023

Ratti, C., Baker, N., & Steemers, K. (2005). Energy consumption and urban texture. Energy and Buildings, 37(7), 762–776. https://doi.org/10.1016/j.enbuild.2004.10.010

Ratti, C., Raydan, D., & Steemers, K. (2003). Building form and environmental performance: Archetypes, analysis, and an arid climate. Energy and Buildings, 35(1), 49–59. https://doi.org/10.1016/S0378-7788(02)00079-8

Rostami, E., Nasrollahi, N., & Khodakarami, J. (2024). A comprehensive study of how urban morphological parameters impact the solar potential, energy consumption, and daylight autonomy in canyons and buildings. Energy and Buildings, 305, 113904. https://doi.org/10.1016/j.enbuild.2024.113904

Sarralde, J. J., Quinn, D. J., Wiesmann, D., & Steemers, K. (2015). Solar energy and urban morphology: Scenarios for increasing the renewable energy potential of neighborhoods in London. Renewable Energy, 73, 10–17. https://doi.org/10.1016/j.renene.2014.06.028

Shi, Z., Fonseca, J. A., & Schlueter, A. (2017). A review of simulation-based urban form generation and optimization for energy-driven urban design. Building and Environment, 121, 119–129. https://doi.org/10.1016/j.buildenv.2017.05.006

Shi, Z., Fonseca, J. A., & Schlueter, A. (2021). A parametric method using vernacular urban block typologies for investigating interactions between solar energy use and urban design. Renewable Energy, 165, 823–841. https://doi.org/10.1016/j.renene.2020.10.067

Stasinopoulos, T. N. (2018). A survey of solar envelope properties using solid modelling. Journal of Green Building, 13(1), 3–30. https://doi.org/10.3992/1943-4618.13.1.3

Tao, Y., Yan, Z., Ni, P., He, B.-J., Qin, G., Yue, Y., Lei, F., Zheng, Z., & Zhang, X. (2025). Capturing available solar energy on urban-scale building surface: A multi-dimensional perspective. Energy and Buildings, 344, 115989. https://doi.org/10.1016/j.enbuild.2025.115989

Thellufsen, J. Z., Lund, H., Sorknæs, P., Østergaard, P. A., Chang, M., Drysdale, D., Nielsen, S., Djørup, S. R., & Sperling, K. (2020). Smart energy cities in a 100% renewable energy context. Renewable and Sustainable Energy Reviews, 129, 109922. https://doi.org/10.1016/j.rser.2020.109922

Tuhus-Dubrow, D., & Krarti, M. (2010). Genetic-algorithm-based approach to optimize building envelope design for residential buildings. Building and Environment, 45(7), 1574–1581. https://doi.org/10.1016/j.buildenv.2010.01.005

Vartholomaios, A. (2015). The residential solar block envelope: A method for enabling the development of compact urban blocks with high passive solar potential. Energy and Buildings, 99, 303–312. https://doi.org/10.1016/j.enbuild.2015.04.046

Vermeulen, T., Merino, L., Knopf-Lenoir, C., Villon, P., & Beckers, B. (2018). Periodic urban models for optimization of passive solar irradiation. Solar Energy, 162, 67–77. https://doi.org/10.1016/j.solener.2018.01.014

Wang, M., Dong, Y., Liao, W., Pan, B., & Li, S. (2025). Impact of residential morphology on outdoor thermal comfort and building energy consumption in winter and summer: A case study. Urban Climate, 61, 102479. https://doi.org/10.1016/j.uclim.2025.102479

Wang, X., Ma, Q., & Duan, Z. (2024). Spatiotemporal effect and influencing factors of total factor energy efficiency: Evidence from urban agglomerations in China. Ecological Indicators, 161, 111984. https://doi.org/10.1016/j.ecolind.2024.111984

York, R., & Bell, S. E. (2019). Energy transitions or additions? Energy Research & Social Science, 51, 40–43. https://doi.org/10.1016/j.erss.2019.01.008

Zhao, H., Yang, R. J., Liu, C., & Sun, Q. (2023). Solar building envelope potential in urban environments: A state-of-the-art review of assessment methods and framework. Building and Environment, 244, 110831. https://doi.org/10.1016/j.buildenv.2023.110831